Production d'énergie (hydraulique, thermique et nucléaire)

CALCULS TRIDIMENSIONNELS D'ECOULEMENTS SOUS UN COUVERCLE DE REACTEUR

3D FLOW COMPUTATIONS UNDER A REACTOR VESSEL CLOSURE HEAD

96NB00122

Direction des Etudes et Recherches

EDF

Electricité de France

Direction des Etudes et Recherches

SERVICE APPLICATIONS DE L'ELECTRICITE ET ENVIRONNEMENT
Département Laboratoire National d'Hydraulique

Décembre 1995

DAUBERT O.
BONNIN O.
HOFMANN F.
HECKER M.

CALCULS TRIDIMENSIONNELS D'ECOULEMENTS SOUS UN COUVERCLE DE REACTEUR

3D FLOW COMPUTATIONS UNDER A REACTOR VESSEL CLOSURE HEAD

Pages : 11

96NB00122

Diffusion : J.-M. Lecœuvre
EDF-DER
Service IPN. Département SID
1, avenue du Général-de-Gaulle
92141 Clamart Cedex

ISSN 1161-0611

SYNTHÈSE :

L'écoulement sous le couvercle de la cuve d'un réacteur à eau pressurisée est étudié à l'aide de plusieurs calculs et d'un modèle physique. L'écoulement présenté ici est turbulent, isotherme et incompressible. Les calculs ont été réalisés avec le code N3S en utilisant un modèle k-ε. Les comparaisons entre les résultats numériques et expérimentaux sont dans l'ensemble satisfaisantes. On prévoit certaines améliorations locales en utilisant soit des modèles de turbulence plus sophistiqués, soit des raffinements du maillage calculés automatiquement à l'aide d'une technique de maillage adaptatif récemment implantée dans N3S pour les cas tridimensionnels.

EXECUTIVE SUMMARY :

The flow under a vessel cover of a pressurised water reactor is investigated by using several computations and a physical model. The case presented here is turbulent, isothermal and incompressible. Computations are made with N3S code using a k-epsilon model. Comparisons between numerical and experimental results are on the whole satisfying. Some local improvements are expected either with more sophisticated turbulence models or with mesh refinements automatically computed by using the adaptive meshing technique which has been just implemented in N3S for 3D cases.

3D FLOW COMPUTATIONS UNDER A REACTOR VESSEL CLOSURE HEAD

by O. DAUBERT, O. BONNIN, F. HOFMANN , M. HECKER -

Electricité de France, Direction des Etudes et Recherches, Laboratoire National d'Hydraulique, 6 quai Watier
78400 CHATOU, FRANCE

I. Introduction

The aim of the study is to determine the incompressible steady flow field under an hemispherical upper closure head of a Pressurised Water Reactor. A lot of vertical tubes, called " adapters " pass through this cover and are weld on it. The control drive rods can move inside the adapters, under the action of electro-magnetic mechanisms.
The fluid domain is partly occupied by vertical guide tubes and thermal sleeves protecting each control rod cluster (fig. 1).
It is necessary to determine the general flow under the cover as well as the local flow inside the adapters. But it is not possible to represent the overall phenomena in a single model. That is why several models are used: two of them are presented here.

II. Organisation of the study

In a first step we compute the general 3D velocity and pressure field, in a 45° of the cover. This geometry is called "COUVERCLE-45°".
The flow in this region is driven by peripheral jets which sweep the internal side of the cover. Flow outlets are located at the top of the 13 guide tubes represented in the model.
The second step is a local 3D computation around an adapter. Boundary conditions are given by the results of the first computation. The flow configuration is more complicated here (fig. 2): the incoming wall flow meets a set of two concentric cylindrical obstacles with an incidence of 48°. It is not a standard flow feature, so the numerical model needs a validation by a physical experiment on the same geometry (fig. 5, 6). This geometry is called "TRAVERSIN".
As the Reynolds number is lower in the experimental model than in the reactor, we use the following procedure:

- in a first time, we try to reproduce the experimental data,
- and in a second one, we impose the real boundary conditions to determine the velocity and pressure fields in and around the adapter.

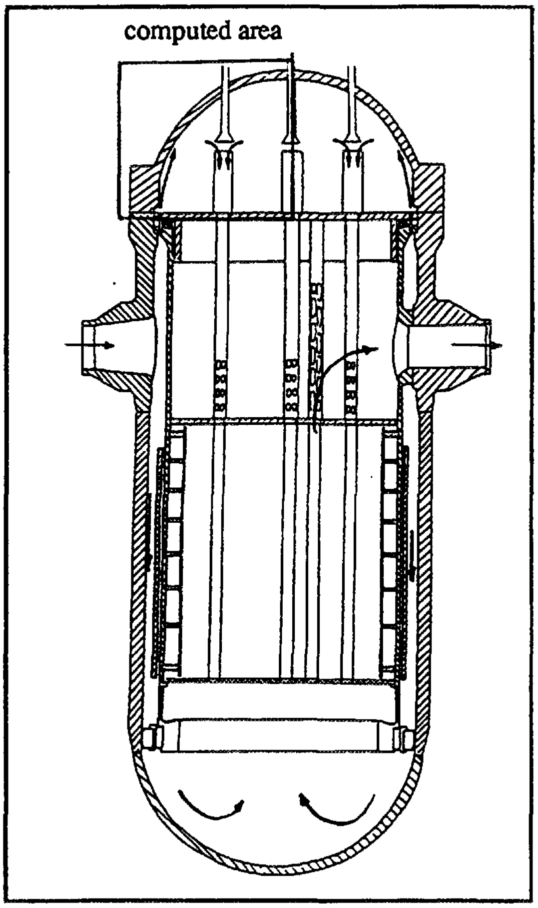

Figure 1 - General view of a pressurised water reactor

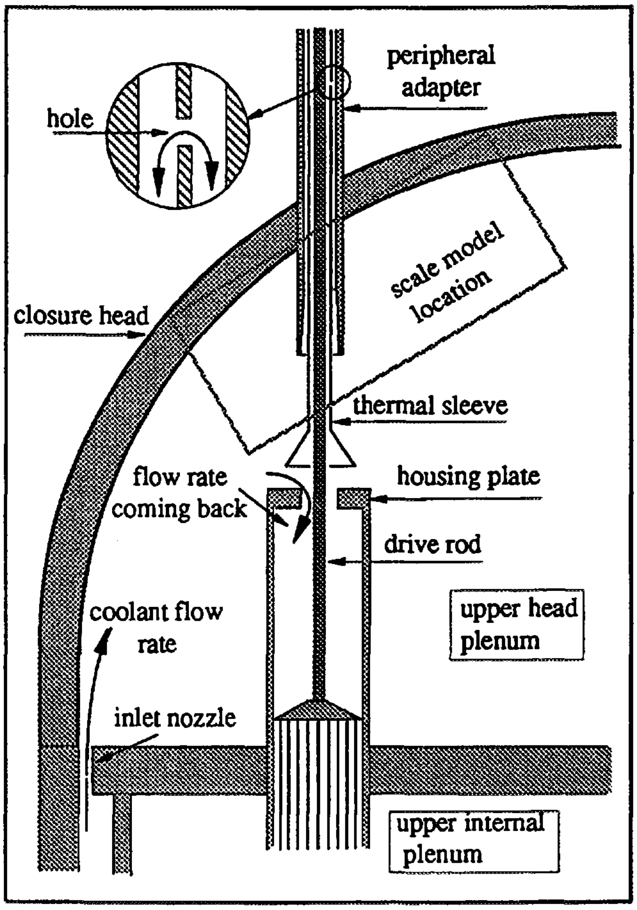

Figure 2 - Global view of the upper head geometry with one adapter

III. The N3S code

N3S is a finite element code developed by EDF for incompressible flow simulations in industrial studies [3]. For code assessment, a wide range of test cases is made under a Quality Assurance procedure for every main release of N3S. Code results are compared with analytical solutions when available or with literature experiments.
Since March 95, version 3.2 have been offering extended capabilities, mainly for compressible flows, coupled thermal computations in fluid and solid [1], and adaptive meshing [2].
In the present study classical Navier-Stokes equations are used with a turbulent viscosity coefficient:

$$\begin{cases} \rho \dfrac{Du}{Dt} = -\nabla p + \nabla \cdot \left[(\mu + \mu_t)(\nabla u + {}^t\nabla u) \right] \\ \nabla \cdot u = 0 \end{cases} \tag{1}$$

In these equations, D/Dt denotes the total derivative in time, u the velocity field, p the pressure, ρ the density, μ the dynamic viscosity, and μ_t the eddy dynamic viscosity coefficient (see below).

The turbulence model used is the $k-\varepsilon$ model for which the turbulent kinetic energy k and dissipation rate ε are the solutions of the following transport-diffusion equations:

$$\begin{cases} \rho\dfrac{Dk}{Dt} = \nabla\cdot\left[\left(\mu+\dfrac{\mu_t}{\sigma_k}\right)\nabla k\right] + P - \rho\varepsilon \\ \rho\dfrac{D\varepsilon}{Dt} = \nabla\cdot\left[\left(\mu+\dfrac{\mu_t}{\sigma_\varepsilon}\right)\nabla \varepsilon\right] + C_{\varepsilon_1}\dfrac{\varepsilon}{k}P + \rho C_{\varepsilon_2}\dfrac{\varepsilon^2}{k} \end{cases} \qquad (2)$$

with: $\mu_t = \rho C_\mu \dfrac{k^2}{\varepsilon}$, $\quad P = 2\mu_t \mathrm{tr}(\mathbf{d}:\mathbf{d})$, $\quad$ and $\quad d_{ij} = \dfrac{1}{2}\left(\dfrac{\partial u_i}{\partial x_j} + \dfrac{\partial u_j}{\partial x_i}\right)$

Various values are given for the coefficients involved in this equations:
in the standard $k-\varepsilon$ model, they are constant. In the RNG model [5, 6], derived according to the renormalization group theory, $C_{\varepsilon 1}$ is no longer a constant but a scalar function of the variable $\eta = (2d_{ij}d_{ij})^{1/2}k/\varepsilon$
Coefficients for both models are given below:

	C_μ	σ_k	σ_ε	$C_{\varepsilon 1}$	$C_{\varepsilon 2}$
standard k-ε	0.09	1	1.30	1.44	1.92
RNG	0.085	0.72	0.72	$1.42 - \dfrac{\eta(1-\eta/4.38)}{1+0.012\eta^3}$	1.68

Appropriate boundary conditions are also defined: for the solid boundaries, a Reichardt law is used (see [3]). Otherwise velocity vectors are prescribed at inlet nodes, and free slip conditions on symmetry planes. For the need of the present study, special treatments for multiple outlets with prescribed normal stress or a pressure-flow rate relation, have been tested in order to validate re-entering flows on some outlets. These tests are excellent for laminar flows, and are slightly penalised, for turbulent flows, by the lack of information on incoming k and ε. Moreover, they show that it is convenient to dispose outlet boundaries far from each others when using pressure-flow rate relations, to avoid instabilities.

These equations and boundary conditions are solved for transient or stationary flows, via a time evolution from initial conditions, generally the rest.
The time discretization is based on a fractional step method involving:

- an advection step, for the non-linear convection terms of the Navier-Stokes, k-ε and eventually temperature equations, solved by a characteristics method,
- a diffusion step for the remaining part of the k and ε equations : the finite element discretization leads to linear systems solved by a preconditioned conjugated gradient algorithm,
- a generalised Stokes problem for the velocity and the pressure, solved by a Chorin algorithm.

The spatial discretization uses P2-P1 or isoP2-P1 tetrahedral elements : pressure is always linear (P1) by element and velocity is quadratic (P2) or piece wise linear (isoP2) ; other scalar variables may be linear, quadratic or piece wise linear.

Adaptive meshing

This method already tested in N3S for 2D flows has been recently available for 3D cases. It needs a local error indicator giving the places where the mesh is too coarse, and a geometrical procedure which refines or de-refines the mesh.

- For turbulent flows, a *projection indicator* is used. It was first introduced in elasticity [4] and then transposed to fluid dynamics. It has been implemented with appropriate adjustments in N3S. It is based on the difference between discrete entities which are discontinuous at the boundary of the elements, and their projection on the functional space of discretization.

For instance, given that $\mathbf{d}_h$ is the discrete tensor calculated using u_h velocity, solution of the discrete problem, and $\mathbf{d}_h^*$ the L^2 projection in the velocity discretization space, the local velocity error indicator, defined for each element K is

$$I_{K,u} = \left(\int_K 2\mu(\mathbf{d}_h - \mathbf{d}_h^*):(\mathbf{d}_h - \mathbf{d}_h^*)d\omega \right)^{½} \qquad (3)$$

As we cannot define a similar indicator by projecting the pressure which is continuous, a L^2 projection Gp_h^* of the discontinuous pressure gradient is calculated in the pressure discretization space. The pressure error indicator is written:

$$I_{K,p} = \left(h_K^2 \int_K \frac{1}{2\mu}(\nabla p_h - G p_h^*)^2 d\omega \right)^{½} \qquad (4)$$

In the general turbulent case, we could also introduce indicators on the turbulent quantities k and ε.
The whole error indicator is written :.

$$I_K = \left(I_{K,u}^2 + I_{K,p}^2 + I_{K,k}^2 + I_{K,\varepsilon}^2\right)^{½} \qquad (5)$$

- The 3D *refinement module* breaks down tetrahedra into eight sub-elements. Mesh conformity is obtained dividing tetrahedra into two or four parts.

IV. Global flow under the cover

- Numerical model COUVERCLE 45°

The upper region of the reactor vessel (fig.1) presents some geometrical symmetry planes, so it is possible to model only a 45° sector of the cover. Nevertheless, only major obstacles are represented in the finite element mesh (fig.3) : it has 140 000 elements and 207 000 velocity nodes (the same domain with all obstacles represented would have about 270 000 elements and 400 000 nodes). There are three peripheral narrow nozzles where the inlet flow is prescribed. Outlets are located inside the 13 guide tubes and their boundary conditions are normal stresses calculated with pressures measured in a previous experimental study (1978) and including the pressure drops of the housing plates. These boundary conditions allow to obtain the flow rate in each guide tube as a result.
The mesh construction is submitted to some criterion, more or less empirical :

- each cylindrical obstacle is discretized by at least 24 circumferential facets,
- along the rigid walls we impose one or more layers of flattened elements, and we take care to have more than one fluid element between two opposite walls,
- special attention is given to the 3 nozzles representation in order to get the right inlet flow rate as well as the real value of the velocities in the potential cone of the 3 jets ; this point leads to very narrow elements in the orthogonal direction of the jets, allowing sharp discontinuities of the incoming velocity profiles,
- but, in the axial direction of the jets, it is better to impose a longer mesh size because of the Courant criterion : $U.\Delta t/\Delta x \approx 1$, which gives an idea of the precision of convective terms. An isotropic mesh would result in a very small time step. In our case, Courant number calculated in the flow direction is less than 2, it is a reasonable value for N3S.

Starting from a null velocity field the simulation is led up to 3100 time steps. They are computed through successive sessions using a restart procedure. The total CPU time is of 32 hours on a CRAY C98. That means a value of 0.17s by time step per 1000 nodes. The steady flow is obtained after about 2000 time steps.

This model gives a good representation of the global flow in the upper head, as it can be seen on the figure 4.

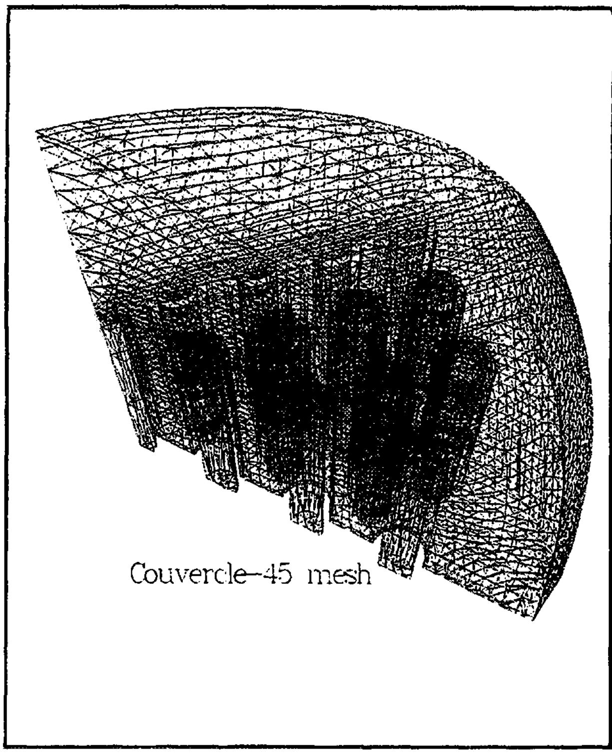

Figure 3 - Finite element mesh of a 45° sector of a reactor upper head

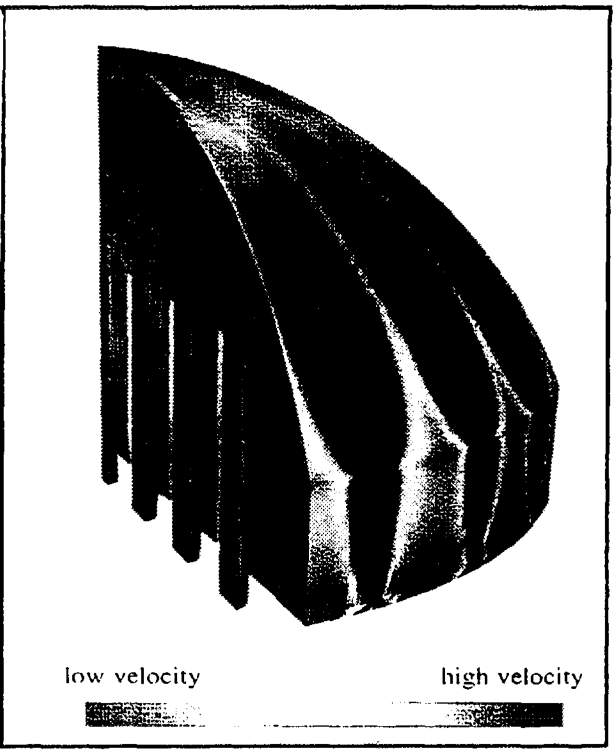

Figure 4 - Velocity field computed in this mesh

V. Local flow around an adapter

- Physical and numerical models TRAVERSIN
Using the results of the previous general flow computation, we have designed a local geometry around a peripheral adapter in order to get precise values of pressure and velocity fields in this area. We want particularly to determine the flow penetration in the annular space between the two concentric cylinders called adapter and thermal sleeve on figure 2.
So we have built a mesh and a scale model on this geometry (fig.5, 6). The scale of the physical model TRAVERSIN is 1 for the length and the velocity, and $1/8^{th}$ for the Reynolds number VD/ν, because of the water viscosity ν which is greater at room temperature than in the reactor. The inlet boundary condition is a velocity profile set by an adjustable guide flow followed by a honey comb which regularises the profile at the entrance of the test section. Pressure taps give the pressure elevation in the annular space with respect to the incident flow.

The mesh (fig.5) used for the numerical model TRAVERSIN has 78 000 tetrahedral elements and 116 000 velocity nodes. This model has the advantage of being free of limitations on the flow rate and the velocity profile at the inlet, but the turbulence model used in the computation has to be tested. From previous test cases, we know that turbulence modelling is not obvious in this type of flow (impinging jet on a cylinder). The comparison between experimental and numerical models is made in the following way:
velocity measurements by laser-Doppler anemometer are done at the entrance of the test section to get the exact 2D velocity profile, and in some planes around the adapter. A time analysis of the velocity measured in a point of the wake doesn't give any Strouhal frequency. So we hope to calculate the steady mean velocity and pressure fields by using a k-ε turbulence model.

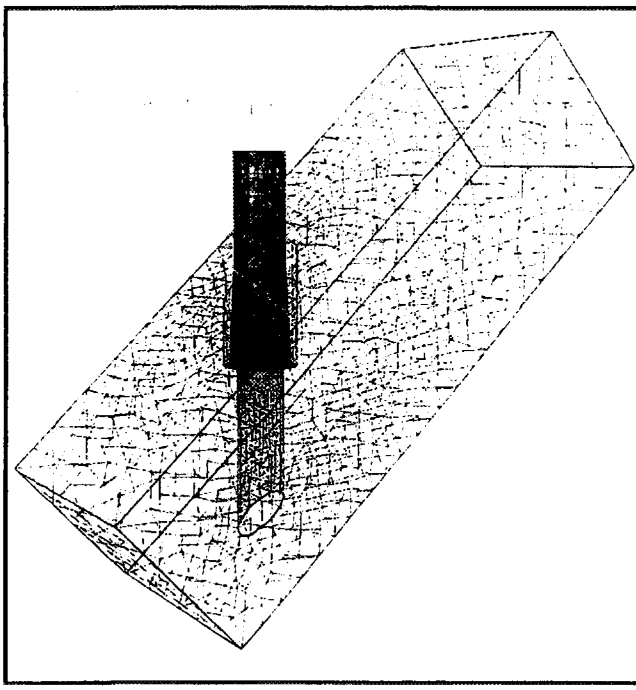

Figure 5 - Mesh of the TRAVERSIN model

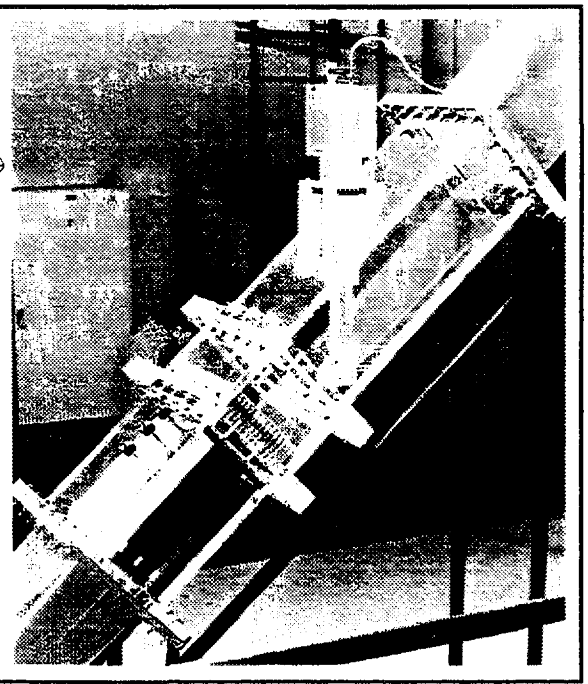

Figure 6 - View of the scale model TRAVERSIN

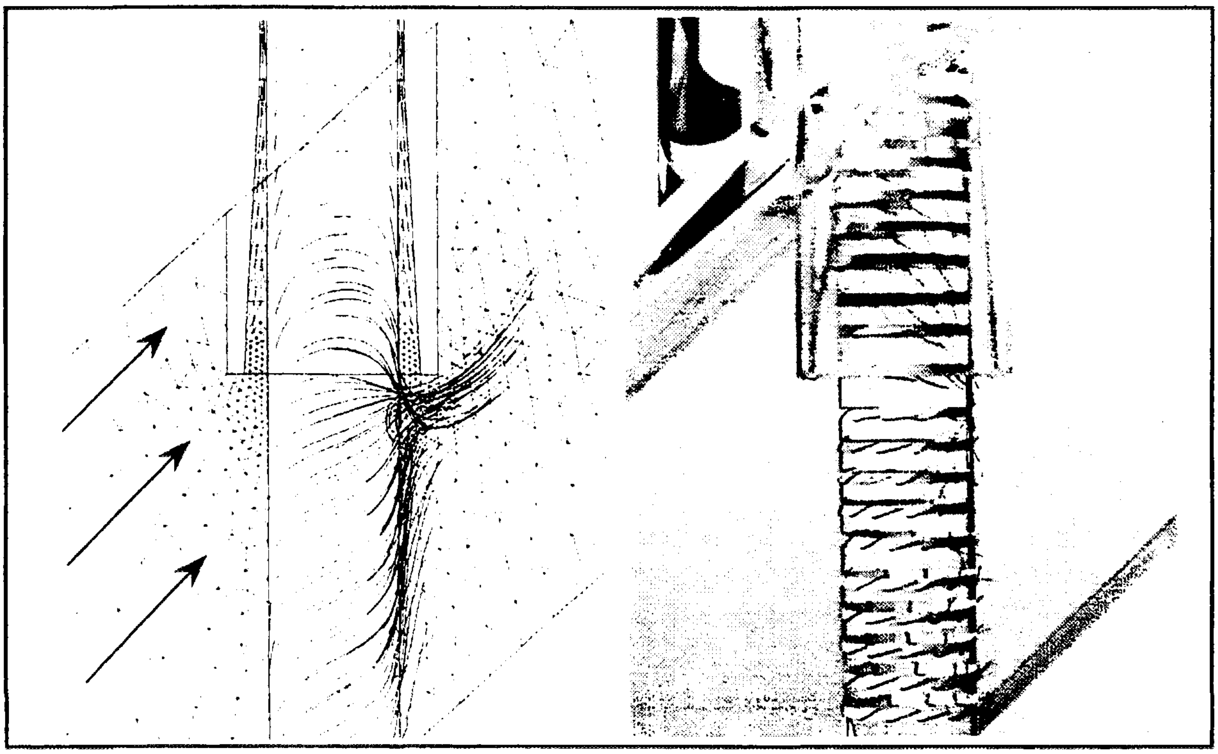

Figure 7 - Comparison between the experimental and numerical TRAVERSIN model

The measured inlet velocity profile is interpolated on the upwind boundary of the mesh with little adjustments to get the right flow rate.
Comparisons with measured velocities in the computed domain are quite good: a very stable horizontal vortex behind the adapter is clearly visible. It should perhaps become more precise with a finer mesh.

The flow penetration in the upper annular channel inside the adapter is visualised in the physical model with wool yarns representing the direction of the velocity vectors. In the numerical one, particle traces are calculated by the post-processor ENSIGHT from the computed velocity field (fig.7). They show the same behaviour, but might be closer on the upwind side. We note also that the computed pressure in the channel is a little lower than the measured one.
It is then interesting to see the both influences of turbulence modelization and mesh refinement. A test made on the same mesh using the modified (RNG) k-ε turbulence model doesn't improve significantly the results ; it will be probably more efficient on a finer mesh.
The adaptive meshing method applied on the previous steady state results gives a first mesh refinement according to the local error indicator The new mesh has 115 000 elements and 169 000 velocity nodes.
To go further in the process more data are needed for the transfer of the boundary conditions on the new nodes created. The only data present in the given input files for this computation are mainly defined by nodal values, and very few information are tight to boundary facets. It is necessary to reconsider the mesh definition in order to characterise more precisely each type of boundary facets and edges.

VI. Conclusion

Numerical 3D flow simulations made with N3S code, give consistent and very useful information about general and local flow under the closure heads of PWR. Thanks to the experimental study lead in parallel with the local flow calculation around an adapter of the cover, one can evaluate the precision of the results. They are really good everywhere, but may be probably enhanced locally by using a method of adaptive meshing with local refinement, and more sophisticated turbulence models as the "RNG k-ε turbulence model" or a Reynolds Stress model "Rij-ε", reducing the energy dissipation at the impact of incident flow on obstacles.

REFERENCES

[1] PENIGUEL C., RUPP I. :
A numerical method for thermally coupled fluid and solid problems.
Proc. of 8th Int. Conf. on Num. Meth. for Thermal Problems, Swansea, U. K., July 1993.

[2] BONNIN O., METIVET B., NICOLAS G., ARNOUX-GUISSE F., LEAL DE SOUSA L. :
Adaptive meshing for N3S fluid mechanics code.
Computational Fluid Dynamics 94, Wiley, p201-208. (1994)

[3] CHABARD J.-P., METIVET B., POT G., THOMAS B. :
An efficient finite element method for the computation of 3D turbulent incompressible flows.
Finite Elements in Fluids, Vol. 8, ed. Wiley (1992).

[4] ZHU J.Z., ZIENKIEWICZ O.C..
Adaptive techniques in the finite element method.
Comm. Appl. Num. Meth., Vol 24, 197-204, 1987

[5] YAKHOT, ORSZAG :
Development of turbulence models for shear flows by a double expansion technique.
Physique of Fluids, July 1992

[6] DURBIN, SPEZIALE :
Local anisotropy in strained turbulence at high Reynolds numbers
Fluids Engineering, n°113 - 1991